

# Analysis of Visible/SWIR surface reflectance ratios for aerosol retrievals from satellite in Mexico City urban area

A. D. de Almeida Castanho<sup>1</sup>, R. Prinn<sup>1</sup>, V. Martins<sup>2,3</sup>, M. Herold<sup>4</sup>, C. Ichoku<sup>3,6</sup>, and L. T. Molina<sup>1,5</sup>

<sup>1</sup>Massachusetts Institute of Technology, USA

<sup>2</sup>JCET, University of Maryland Baltimore County, USA

<sup>3</sup>NASA/Goddard Space Flight Center, Greenbelt, Maryland, USA

<sup>4</sup>Friedrich-Schiller-University Jena, Germany

<sup>5</sup>Molina Center for Energy and the Environment, USA

<sup>6</sup>University of Maryland, College Park, Maryland, USA

Received: 16 April 2007 – Published in Atmos. Chem. Phys. Discuss.: 11 June 2007

Revised: 21 September 2007 – Accepted: 18 October 2007 – Published: 25 October 2007

**Abstract.** The surface reflectance ratio between the visible (VIS) and shortwave infrared (SWIR) radiation is an important quantity for the retrieval of the aerosol optical depth ( $\tau_a$ ) from the MODIS sensor data. Based on empirically determined VIS/SWIR ratios, MODIS  $\tau_a$  retrieval uses the surface reflectance in the SWIR band ( $2.1\ \mu\text{m}$ ), where the interaction between solar radiation and the aerosol layer is small, to predict the visible reflectances in the blue ( $0.47\ \mu\text{m}$ ) and red ( $0.66\ \mu\text{m}$ ) bands. Therefore, accurate knowledge of the VIS/SWIR ratio is essential for achieving accurate retrieval of aerosol optical depth from MODIS. We analyzed the surface reflectance over some distinct surface covers in and around the Mexico City metropolitan area (MCMA) using MODIS radiances at  $0.66\ \mu\text{m}$  and  $2.1\ \mu\text{m}$ . The analysis was performed at  $1.5\ \text{km} \times 1.5\ \text{km}$  spatial resolution. Also, ground-based AERONET sun-photometer data acquired in Mexico City from 2002 to 2005 were analyzed for aerosol depth and other aerosol optical properties. In addition, a network of hand-held sun-photometers deployed in Mexico City, as part of the MCMA-2006 Study during the MILAGRO Campaign, provided an unprecedented measurement of  $\tau_a$  in 5 different sites well distributed in the city. We found that the average RED/SWIR ratio representative of the urbanized sites analyzed is  $0.73 \pm 0.06$  for scattering angles  $< 140^\circ$  and goes up to  $0.77 \pm 0.06$  for higher ones. The average ratio for non-urban sites was significantly lower (approximately 0.55). In fact, this ratio strongly depends on differences in urbanization levels (i.e. relative urban to vegetation proportions and types of surface materials). The aerosol optical depth retrieved from MODIS radiances at a spatial resolution of  $1.5\ \text{km} \times 1.5\ \text{km}$

and averaged within  $10 \times 10\ \text{km}$  boxes were compared with collocated 1-h  $\tau_a$  averaged from sun-photometer measurements. The use of the new RED/SWIR ratio of 0.73 in the MODIS retrieval over Mexico City led to a significant improvement in the agreement between the MODIS and sun-photometer AOD results; with the slope, offset, and the correlation coefficient of the linear regression changing from ( $\tau_{\text{aMODIS}} = 0.91 \tau_{\text{a sun-photometer}} + 0.33$ ,  $R^2 = 0.66$ ) to ( $\tau_{\text{aMODIS}} = 0.96 \tau_{\text{a sun-photometer}} - 0.006$ ,  $R^2 = 0.87$ ). Indeed, an underestimation of this ratio in urban areas lead to a significant overestimation of the AOD retrieved from satellite. Therefore, we strongly encourage similar analyses in other urban areas to enhance the development of a parameterization of the surface ratios accounting for urban heterogeneities.

## 1 Introduction

Monitoring the atmospheric composition in megacities around the world and understanding the impact of the emitted pollutants on the local air quality and global climate remains a challenge for the scientific community. The air quality monitoring systems in most megacities have relied almost exclusively on ground-based station networks, which do not provide adequate spatial coverage. Satellites provide a systematic observation of more spatially continuous aerosol properties that are complementary to in situ measurements (Al Saadi et al., 2005; Li et al., 2005). The aerosol optical depths ( $\tau_a$ ) retrieved at  $10\ \text{km}$  spatial resolution from the Moderate-Resolution Imaging Spectro-radiometer (MODIS) sensor onboard the Terra and Aqua satellites are already providing important information on global aerosol climatology

Correspondence to: A. D. de Almeida Castanho  
(castanho@mit.edu)

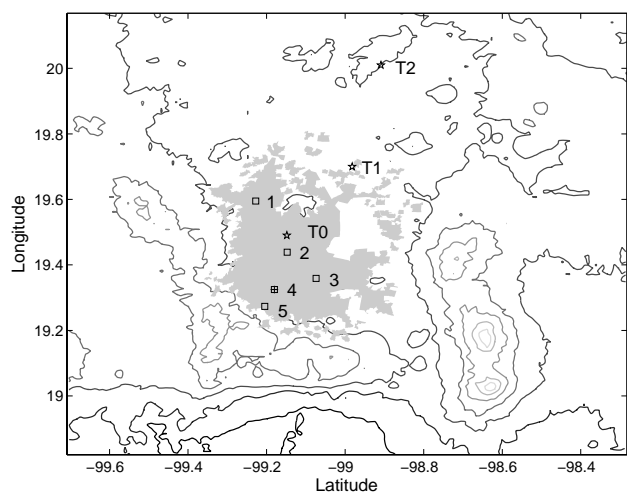


**Fig. 1.** Map indicating: (\*) the MILAGRO 2006 super sites T0, T1 and T2; (□) and the sun-photometer network, where (1) Tec, (2) Hidalgo Metro Station-Mexico City, (3) UAM-I, (4) UNAM and (5) Corena; (+) AERONET site location at UNAM during 2002–2005.

(Remer, et al., 2005). With the growing concern of the emissions of particulate matter in megacities, there is increased interest in higher resolution  $\tau_a$  data from satellite retrievals. Such higher resolution data will be helpful to describe the detailed distribution of the pollution plume in cities, and aid in air quality monitoring and forecasting. Higher spatial resolution can also help to better understand the direct or indirect radiative effects of aerosol plumes in urban areas and to illuminate research on how the urban aerosol plumes contribute to climate impacts on the global scale. However, to achieve a higher spatial resolution in  $\tau_a$  retrieval from the MODIS instrument over urban areas, it is essential to have more accurate information on the surface reflectance and aerosol optical properties.

Sensitivity studies performed in this work for  $\tau_a$  estimates show that an error of  $\pm 10\%$  on a surface reflectance ( $\rho_{\text{surf}}$ ) of 0.15 at 2.1  $\mu\text{m}$  wavelength can introduce an error in  $\tau_a$  of up to 65% when  $\tau_a$  values are around 0.2. The sensitivity of  $\tau_a$  to surface reflectance decreases for higher  $\tau_a$  values, although it increases as a function of the surface reflectance. Mexico City has a surface reflectance that ranges from 0.1 to 0.25 at 2.1  $\mu\text{m}$  wavelength, which is close to the acceptable limit in the standard MODIS aerosol retrieval algorithm over land ( $\rho_{\text{surf}}(2.1 \mu\text{m})=0.25$ ) (King et al., 2003; Remer et al. 2005).

Kaufman et al. (1997b) empirically derived a strong correlation between some visible (VIS) and short-wave infrared (SWIR) wavelength bands over vegetated and dark soil surfaces ( $\rho_{\text{surf}}(0.47 \mu\text{m})=0.25*\rho_{\text{surf}}(2.1 \mu\text{m})$  and  $\rho_{\text{surf}}(0.66 \mu\text{m})=0.5*\rho_{\text{surf}}(2.1 \mu\text{m})$ ). Kaufman et al. (2002) provide a physical explanation for these VIS/SWIR ratios, which are a key parameter used in the MODIS algorithm

to compute  $\tau_a$  over land. The ratio is used to estimate the surface reflectance in the visible (0.66 and 0.47  $\mu\text{m}$ ) wavelengths based on the radiance measured at 2.1  $\mu\text{m}$  wavelength. The non-Lambertian behavior of the land surfaces is represented by the Bi-directional Reflectance Distribution Functions (BRDF) that vary with wavelength and differences in surface types, which in turn influence the VIS/SWIR ratios. Levy et al. (2007) performed extensive analyses on the VIS/SWIR ratios globally at several Aerosol Robotic Network (AERONET) sites. Their work evaluated the principal trends of this ratio and expressed it as a function of scattering angle (Gatebe et al., 2001; Remer et al., 2001) and Normalized Difference Vegetation Index defined with short wave infrared wavelength (NDVI swir).

The heterogeneity of the surface cover in an urban environment only increases the uncertainties in the estimation of the VIS/SWIR ratios. Reducing the uncertainties involved in estimating these ratios in urban areas is a critical issue in the  $\tau_a$  retrieval from satellites (Gross et al., 2005). In this work, we analyzed an unprecedented measurement of  $\tau_a$  from a network of sun-photometers deployed in Mexico City during the MILAGRO (Megacity Initiative: Local and Global Research Observations) Campaign in 2006 as part of the MCMA-2006 Study (see <http://mce2.org>). The detailed analysis enabled the determination of a new  $\rho_{\text{surf}}(0.66)/\rho_{\text{surf}}(2.1)$  ratio for an urban area like Mexico City. We also present the improvement that the new ratio estimate can yield for  $\tau_a$  retrievals over the city.

## 2 The MILAGRO Field Campaign, Instruments, and Measurements

The MILAGRO Campaign was carried out during the month of March 2006 in and around the Mexico City metropolitan area (<http://www.eol.ucar.edu/projects/milagro>). The Campaign was designed to better understand the local, regional and global impact of pollutants generated in megacities, ranging from the health effects through the induced climate change. The MILAGRO field experiment involved more than 400 researchers from over 120 institutions in the USA, Mexico, and several other countries. It had four main components: the MCMA-2006 (Mexico City Metropolitan Area – 2006) led by the Molina Center for Energy and the Environment, the MAX-Mex (Megacity Aerosol Experiment in Mexico City) led by the U.S. Department of Energy (DOE) Atmospheric Science Program (ASP), the MIRAGE-Mex (Megacity Impacts on Regional and Global Environments) led by the National Center for Atmospheric Research (NCAR), and the INTEX-B (Intercontinental Chemical Transport Experiment Phase B) led by NASA. The Campaign involved coordinated aircraft and ground-based measurements supported by extensive modeling and satellite observations. The ground-based measurements were concentrated in 3 main supersites; one in the urban area of Mexico City called T0 and the other two

(T1 and T2) were located outside of the city toward the northeast, as shown in Fig. 1. The locations were strategically selected to characterize the transport and transformation of the pollutants exported from the urban area of the city.

The Moderate Resolution Imaging Spectroradiometer (MODIS) is a sensor aboard the Terra and Aqua satellites launched by NASA in December 1999 and May 2002, respectively (King et al., 2003; Parkinson, 2003). Both satellites are operating in a sun-synchronous orbit providing data with near daily global coverage, with equator crossing at approximately 10:30 a.m. and 1:30 p.m. local times (Terra and Aqua satellites respectively).

In this work, we use MODIS upward reflectance measurements calibrated and geolocated, and made available as a Level 1B product (King et al., 2003). We have used the reflectances provided at 500 m resolution for channels centered at 0.47, 0.55, 0.66, 0.86, 1.24, 1.64 and 2.13  $\mu\text{m}$ . Uncertainties in the measured reflectance in the visible and mid-IR are less than 2% (Guenther et al., 2002). All MODIS reflectance data acquired over Mexico City from 2002 to 2005 and also for the period of March 2006 were analyzed.

The AERONET is a global ground-based network of sun/sky automated radiometers (CIMEL Eletronique 318A, France) supported by NASA's Earth Observing System (EOS) and other international institutions (Holben et al., 2001). The instrument makes direct sun radiance measurements every 15 minutes and sky-measurements every hour. The AERONET instrument measures  $\tau_a$  with an accuracy of  $\pm 0.01$  (Holben et al., 2001), using solar direct radiance measurements at 1.02, 0.870, 0.670, 0.500, 0.440, 0.380 and 0.340  $\mu\text{m}$ . AERONET instruments also provide the aerosol volume size distribution and refractive indices at 1.02, 0.870, 0.670 and 0.440  $\mu\text{m}$  based on sky-radiance measurements at several angles (Dubovik and King, 2000).

The Mexico City AERONET station has been operated continuously since 1999 at the Universidad Nacional Autonoma de Mexico (UNAM), whose location is shown in Fig. 1. During the MCMA-2006 Study, the instrument was moved to the T0 supersite located at IMP (Instituto Mexicano del Petroleo) and operated from 2 March to 18 April 2006 (Fig. 1). In addition, there were two other AERONET instruments located at T1 and T2 (Fig. 1). These represent non-urban areas located at approximately 30 and 60 km respectively toward the northeast from T0. This work uses the AERONET data acquired at UNAM during 2002–2005, and at T0, T1 and T2 for the whole period of March 2006. Besides the aerosol optical depth, the AERONET (UNAM1999–2005) also provided the aerosol optical properties which we used in this work to define the aerosol optical models (single scattering albedo ( $\omega_o$ ), asymmetry parameter ( $g$ ) and extinction efficiency ( $Q_{\text{ext}}$ )).

## 2.1 The Microtops II sun-photometer network measurements

A network of Microtops II sun-photometers was set up in the Mexico City metropolitan area during the MILAGRO Campaign as part of the MCMA-2006 Study. The Microtops II is a handheld sun-photometer manufactured by the Solar Light Company, Philadelphia, USA (Morys et al., 2001). The sun-photometer measures solar radiance at five spectral wavelengths that range from the ultraviolet to the SWIR. The filters used in all channels have a peak wavelength precision of  $\pm 1.5$  nm, and a full width at half maximum (FWHM) band pass of 10 nm. A calibrated Microtops II retrieval of  $\tau_a$  can be considered accurate to within  $\pm 0.03$  (Ichoku et al., 2002b). The physical and operational characteristics of the instrument are detailed in the "User's Guide," which is publicly accessible on the Internet (<http://www.solar.com/manuals.htm>). The main advantage in the use of the Microtops II instrument is its easy operation, mobility, and stability of the measurements. These instruments have been used previously in several field experiments designed to validate satellite  $\tau_a$  retrievals (Ichoku et al., 2002a; Levy et al., 2005).

We operated 5 Microtops II instruments measuring  $\tau_a$  in visible wavelengths at 5 locations distributed in the urbanized area. Most of the instruments started measurements on 5 March and finished on 28 March. The characteristics, serial number, location coordinates and period of operation of each one of the Microtops II instruments, as well as the AERONET instruments are listed in Table 1, and their locations are also shown in Fig. 1.

The sites called TEC (Tecnologico de Monterrey) in the northwest, UAM-I (Universidad Autonoma Metropolitana at Iztapalapa) in the southeast and UNAM in the west were located at a minimum distance of 10 km from the main supersite T0 in the urbanized area. The site here called Hidalgo is located close to the metro station with the same name located close to downtown historical center in Mexico City. It was chosen to characterize the main downtown conditions. The last site called Corena represents the southwestern border of the city characterized by a vegetated landscape. The measurements were taken every sunny day, from 09:45 a.m. until 2:45 p.m., including weekends. The interval between measurements was usually 15 minutes. However a greater time resolution of 5 minutes was used for  $\pm 1.5$  h around the Terra and Aqua overpass times. Each Microtops II data point consisted of 3 consecutive measurements, designed to retain the data with the best alignment of the instrument line of sight with the Sun.

The procedure used in the  $\tau_a$  computation was the same as the one described in detail by Ichoku et al. (2002b). The  $\tau_a$  was recalculated based on the measured voltages, and considering the Rayleigh and ozone atmospheric corrections and new calibration coefficients. The calibration coefficient at a given wavelength for a particular instrument represents the

**Table 1.** Characteristics of the sun-photometer instruments used in the 2006 MILAGRO campaign in Mexico City. Only the wavelengths in bold on the Microtops II instruments were calibrated.

Sun-photometer	Location	Wavelength ( $\mu\text{m}$ )	Coordinates	Altitude (m)	Start/end 2006
Microtops II 3762	Hidalgo Metro Station Mexico City	0.34; <b>0.44</b> ; <b>0.67</b> ; <b>0.87</b> ; 0.93	19.44° N –99.15° W	2260	13-March 28-March
Microtops II 3763	UNAM	0.34; <b>0.44</b> ; <b>0.67</b> ; <b>0.87</b> ; 0.93	19.32° N –99.18° W	2300	5-March 28-March
Microtops II 5378	Corena	<b>0.44</b> ; <b>0.87</b> ; 0.93; 1.64; 2.10	19.27° N –99.20° W	2570	6-March 28-March
Microtops II 5379	Technol. Monterrey	<b>0.44</b> ; <b>0.87</b> ; 0.93; 1.64; 2.10	19.59° N –99.23° W	2350	5-March 28-March
Microtops II 5376	UAM-I	0.38; <b>0.50</b> ; <b>0.67</b> ; <b>0.87</b> ; 1.64	19.36° N –99.07° W	2250	5-March 28-March
CIMEL AERONET	T0	<b>0.34</b> ; <b>0.38</b> ; <b>0.44</b> ; <b>0.50</b> ; <b>0.67</b> ; <b>0.87</b> ; <b>1.02</b>	19.49° N –99.15° W	2257	5-March 28-March
CIMEL AERONET	T1	<b>0.34</b> ; <b>0.38</b> ; <b>0.44</b> ; <b>0.50</b> ; <b>0.67</b> ; <b>0.87</b> ; <b>1.02</b> ; <b>1.64</b>	19.70° N –98.98° W	2272	5-March 28-March
CIMEL AERONET	T2	<b>0.44</b> ; <b>0.67</b> ; <b>0.87</b> ; <b>1.02</b>	20.0° N –98.91° W	2542	5-March 28-March

extraterrestrial signal at that wavelength. The calibration of each instrument was done by relative calibration against the AERONET radiometer in operation in Mexico City at T0, based on the calibration methodology described by Ichoku et al. (2002b). The calibrations were performed when there was no cloud cover during 2, 3 and 4 March, just prior to deployment and also on 25, 26 and 27 March post-deployment. The calibrations were done strategically at the beginning and at the end of the experiment to account for any change in the calibration coefficient. However, it was found that the calibration coefficients were stable for all the instruments during the period of the experiment.

### 3 Quality assurance of the reflectance at the top of the atmosphere (TOA)

A cloud mask was applied on the MODIS reflectance data (Level 1B) at 500 m resolution using a method similar to the procedure described by Martins et al. (2002). In this process, we computed the standard deviation of the reflectance at 0.66  $\mu\text{m}$  for each group of  $3 \times 3$  pixels, and discarded the groups with standard deviation larger than 0.01 (which is the threshold used to identify the possibility of cloud contamination). To avoid residual contamination from cloud remnants, cloud shadows, or very bright surfaces, we also discarded pixels whose measured reflectance at 2.1  $\mu\text{m}$  was smaller than 0.01 or larger than 0.25, as is also done in the MODIS operational algorithm (Remer et al., 2005; Levy et al., 2007). In addition, for each  $3 \times 3$  set of pixels, we also discarded the darkest and the 4 brightest pixels at 0.66  $\mu\text{m}$  to avoid any

other possibility of influence by clouds or water bodies still remaining in the dataset. Although this asymmetric filtering approach appears to give preference to the darker pixels, it was compared to more symmetric approaches and found not to introduce any bias in the retrieved surface reflectance ratios or AOD. The remaining pixels were averaged to simulate the surface reflectance at 1.5 km resolution. Furthermore, the parts of the MODIS images acquired with sensor zenith angles greater than  $40^\circ$  were excluded from the analyses to avoid any extra issues arising from satellite image wing effects.

### 4 The aerosol optical model defined for Mexico City

We have defined a set of aerosol optical models that represent the heterogeneity of the aerosols over the Mexico City area. The aerosol optical properties were analyzed using AERONET measurements from 2002 to 2005. Performing a cluster analysis, we identified 5 aerosol optical models based on the spectral single scattering albedo (at the four wavelengths: 1.02, 0.87, 0.67, 0.47  $\mu\text{m}$ ). The 5 aerosol optical models were defined by an average of the optical properties in each identified cluster. The optical properties that define an aerosol optical model are the single scattering albedo ( $\omega_o(\lambda)$ ), the phase function ( $P(\Theta, \lambda)$ ) and the extinction efficiency ( $Q_{\text{ext}}(\lambda)$ ), shown in Table 2. We used a Henyey-Greenstein approximation for the phase function, defined by the asymmetry parameter ( $g(\lambda)$ ). The 5 aerosol models were not equally distributed; most of the cases were concentrated on aerosol model 4 which makes the average of all the

**Table 2.** Spectral optical properties (Single Scattering Albedo ( $\omega_o$ ); Asymmetry Parameter ( $g$ ); Extinction Coefficient ( $Q_{\text{ext}}$ )) of the 5 aerosol optical models derived from the AERONET database (UNAM 1999–2005). Aerosol model number four used in this work is shown shaded.

#	$\lambda$ ( $\mu\text{m}$ )	0.44	0.55	0.67	0.87	1.02
Aerosol	$\omega_o(\lambda)$	0.77±0.06	0.74±0.05	0.72±0.05	0.65±0.06	0.62±0.06
Model 1	$g(\lambda)$	0.66±0.05	0.62±0.05	0.59±0.05	0.58±0.05	0.58±0.05
(315)	$Q_{\text{ext}}(\lambda)$	1.6±0.1	1.00	0.77±0.04	0.58±0.08	0.5±0.1
Aerosol	$\omega_o(\lambda)$	0.84±0.03	0.82±0.02	0.81±0.02	0.76±0.02	0.74±0.03
Model 2	$g(\lambda)$	0.66±0.04	0.63±0.04	0.60±0.04	0.58±0.04	0.58±0.05
(563)	$Q_{\text{ext}}(\lambda)$	1.6±0.1	1.00	0.77±0.03	0.56±0.07	0.48±0.09
Aerosol	$\omega_o(\lambda)$	0.87±0.02	0.86±0.02	0.85±0.02	0.82±0.02	0.81±0.03
Model 3	$g(\lambda)$	0.66±0.04	0.63±0.04	0.60±0.04	0.57±0.04	0.57±0.05
(658)	$Q_{\text{ext}}(\lambda)$	1.6±0.1	1.00	0.77±0.03	0.54±0.08	0.5±0.1
Aerosol	$\omega_o(\lambda)$	0.91±0.02	0.90±0.02	0.90±0.02	0.88±0.03	0.87±0.03
Model 4	$g(\lambda)$	0.67±0.05	0.64±0.05	0.61±0.05	0.58±0.05	0.57±0.05
(1142)	$Q_{\text{ext}}(\lambda)$	1.5±0.1	1.00	0.77±0.04	0.53±0.08	0.4±0.1
Aerosol	$\omega_o(\lambda)$	0.98±0.01	0.98±0.02	0.98±0.02	0.97±0.02	0.97±0.02
Model 5	$g(\lambda)$	0.68±0.06	0.65±0.05	0.62±0.06	0.59±0.06	0.58±0.06
(607)	$Q_{\text{ext}}(\lambda)$	1.6±0.2	1.00	0.74±0.06	0.5±0.1	0.4±0.1

aerosol models closer to aerosol model 4 than to any other. In this work, we therefore chose to use aerosol model 4, hereafter called the MX (Mexico City) aerosol model.

At 0.55  $\mu\text{m}$  the MX aerosol model has an average single scattering albedo of  $0.90\pm 0.02$  and asymmetry parameter of  $0.64\pm 0.05$ , which are in agreement with the statistical analyses performed by Dubovik et al. (2002) for Mexico City. The average  $\omega_0$  of Mexico City aerosols is higher than that of Sao Paulo ( $0.85\pm 0.01$ ) but lower than that of the urban pollution in Washington D.C. ( $0.98$ ). The differences between the absorption and scattering properties of the particles result from several factors, but the most relevant factor is the different black carbon concentration in each of the regions (Dubovik et al., 2002, Castanho et al., 2005, Salcedo et al., 2006). As presented in those studies, black carbon represents 21% of the fine mode of the aerosol mass concentration ( $\text{PM}_{2.5}$ ) in Sao Paulo, about 3% of  $\text{PM}_{2.5}$  in the east coast of USA, and 11% of  $\text{PM}_{2.5}$  in Mexico City.

## 5 Estimation of the surface reflectance

To estimate the surface reflectance ( $\rho_{\text{surf}}$ ) from satellite data, the top of the atmosphere (TOA) radiance signal has to be corrected for atmospheric gas absorption and Rayleigh scattering, and aerosol scattering and absorption (Vermote, 1997). This correction eliminates the effects of atmospheric interaction with the radiation, leaving the radiation that would be reflected only by the surface (Kaufman et al., 1997a). For accurate correction, it is important to know accurately the aerosol optical depth, aerosol optical properties (single scattering albedo, asymmetry parameter, and extinc-

tion efficiency), and atmospheric water vapor and other trace gas concentrations.

In this work, we used real time information on the aerosol optical depth from radiometric measurements with the ground-based sun-photometer network. The water vapor contents were also derived from real time data measured by the AERONET instrument at T0. Aerosol optical properties were defined using the AERONET database as described in the previous section. We used the tropical region climatological temperature and gas profiles from the SBDART library, corrected for the Mexico City elevation, which is around 2240 m above sea level. We used for each day an average of the sensor and solar zenith and azimuth angles for all the pixels in the Mexico City area (that covers an area smaller than one degree latitude and longitude). This is an approximation that does not significantly affect the optical depth estimates. The inversion equations expressing the surface reflectance as a function of the TOA reflectance were defined from simulations using the SBDART radiative transfer code (Ricchiuzzi et al., 1998). The equations were defined using parameters representative of the relevant conditions described above (water vapor, geometry) for each day for different  $\tau_a$ . Once the TOA reflectance was obtained from the satellite and  $\tau_a$  was measured by sun-photometer, the equation generated gives us the corresponding value of the surface reflectance.

The surface reflectance used in this work was estimated from MODIS quality-assured TOA reflectances (see Sect. 3 for quality assurance details used in this work) at 1.5 km spatial resolution and at 0.47, 0.66 and 2.1  $\mu\text{m}$  wavelengths. We calculated surface reflectances for each 1.5 km  $\times$  1.5 km pixel within the 10 km box that was centered on each sun-

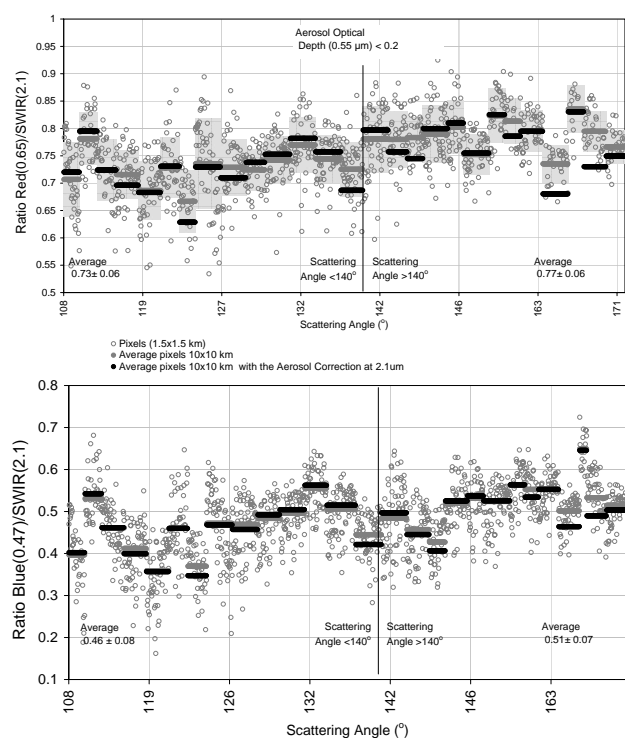


**Fig. 2.** Ratio between surface reflectivities at: (a) 0.66 and 2.1  $\mu\text{m}$  and (b) 0.47 and 2.1  $\mu\text{m}$ , for  $\tau_a$  smaller than 0.2, as a function of scattering angle. Open circles represent the individual ratio for each pixel (1.5 km  $\times$  1.5 km) within a 10 km box around the AERONET site at UNAM (2002–2005). The average and standard deviation for each day (within the 10-km box) are represented by grey circles and bars respectively. Black bars represent the averages for each day (within the 10 km box) of the surface ratio estimation for correcting the aerosol effect at 2.1  $\mu\text{m}$ .

photometer deployed. The quantity  $\rho_{\text{surf}}(0.66)/\rho_{\text{surf}}(2.1)$  corresponds to the ratio of the estimated surface reflectance at 0.66 and 2.1  $\mu\text{m}$  wavelengths in each pixel.

### 5.1 Results and discussion of the surface reflectance estimation

Figure 2 shows the VIS/SWIR ratios for all the days (27) in the period from 2002 to 2005 over the AERONET site at UNAM that met the following predefined conditions: days with no cloud contamination, sensor zenith angle  $<40^\circ$ , and days with  $\tau_a$  from AERONET smaller than 0.2 at 0.55  $\mu\text{m}$ . These conditions were intended to minimize errors from assumptions on atmospheric correction (multiple scattering by the aerosol layer) and, therefore, uncertainties on the surface reflectance estimation. We also indicate the days with scattering angle  $>140^\circ$  to show that the angular geometry influences the surface reflectance as well as the ratio, as discussed by Gatebe et al. (2001) and Remer et al. (2001). However, the full BRDF effect over Mexico City is expected to be ad-

ressed by the Cloud Absorption Radiometer flown aboard the NASA's Jetstream-31 aircraft during MILAGRO. Such a study will be able to provide more information on the angular dependence of the surface reflectance over the urban area.

Figure 2a shows the ratios derived over this region. The red ratio ( $\rho_{\text{surf}}(0.66)/\rho_{\text{surf}}(2.1)$ ) is on average  $0.73 \pm 0.06$  for scattering angles lower than  $140^\circ$  and increases to  $0.77 \pm 0.06$  on average for scattering angles higher than  $140^\circ$ . The positive dependence of the ratio on the scattering angle is in agreement with the tendency observed in general for different regions around the world (Levy et al., 2007). However, the surface ratio observed in Mexico City is higher compared to the average values (varying from 0.4 to 0.6 for scattering angles lower and higher than  $140^\circ$  respectively) estimated in MODIS operational (Level 2 Collection 5) product (Levy et al., 2007). The MODIS operational algorithm still underestimates the ratios specifically for urban areas, although it was not designed for highly urbanized areas without vegetation. Gross et al. (2005) also found values that ranged from 0.6 to 0.7 from low to high urbanized regions in New York. Underestimation of the surface ratio produces an overestimation of  $\tau_a$  retrieved from MODIS and its effect is shown in Sect. 6. Therefore, this is an important issue that has to be taken into account when detailed studies are conducted over urban areas.

Figure 2b shows the results for the blue ratio ( $\rho_{\text{surf}}(0.47)/\rho_{\text{surf}}(2.1)$ ). In general, the blue ratio presented systematically higher values (0.4–0.6) compared to the global average (0.25–0.3) (Levy et al., 2007). It also shows a positive dependence on the scattering angle and a high daily and spatial variability. The best fit for the blue scale, though is the linear fit and the constant factor is not negligible. The linear fit between  $\rho_{\text{surf}}(0.47)$  and  $\rho_{\text{surf}}(2.1)$  resulted in a slope of 0.65 and an offset of 0.025 ( $r^2=0.6$ ). The blue ratio plot shows more noise than the red channel as observed in previous work (Remer et al., 2005, Levy et al., 2004). Levy et al., 2004 showed that neglecting the effects of the polarization at the blue channel is a source of noise in short term analyses. Since the polarization effect is not being considered in the current analysis, the results for the blue channel are likely to contain greater uncertainty, and may not meet the level of accuracy necessary in this type of study. Therefore, the blue ratio results are presented in Figure 2b is shown just as a reference, and will not be emphasized in the following analyses.

The reflectance of an aerosol layer at 2.1  $\mu\text{m}$  is significant when there is a substantial coarse mode fraction in the atmosphere. To test for possible interference by the coarse mode on the ratios derived in this analysis we examined the correction of the aerosol layer in the atmosphere at 2.1  $\mu\text{m}$ . Using  $\tau_a$ , we defined aerosol models based on aerosol optical properties measured by the AERONET sun-photometer in a 4-h interval around the satellite overpass time. The real-time measurements were used to get as close as possible to the real condition of the atmosphere. New look-up tables

were generated specifically for each day to correct for the aerosol layer effect at  $2.1 \mu\text{m}$ . The average ratio obtained with this correction for each day is presented (as black bars) in Fig. 2, which shows that the difference between the corrected and uncorrected ratios is less than 4% for the majority of the cases. This confirms that the  $\rho_{\text{surf}}(0.66)/\rho_{\text{surf}}(2.1)$  ratio deduced for Mexico City is not an artifact of any atmospheric aerosol effect on the estimated surface reflectance. However, there is a significant variability in the ratio from one day to another. These variations can be related to different observation geometries: sun/sensor view zenith and azimuth angles. The urban surfaces are generally non-Lambertian (Meister, 2000). While some targets show forward-scattering behavior, others show stronger backscattering behavior. When such characteristics are added to the spectral dependence and the composition of different surface types within a 10-km spatial average, the resultant effect can contribute to the high variability observed in the ratio. The differences can also be related to variations in soil humidity, shadows, and aerosol optical model assumptions that would need to be analyzed further.

The open circles in Fig. 2 represent the estimates for each pixel (1.5 km spatial resolution) in a 10-km box, for each day. Note that even within a single 10-km box there is a high variability of the ratios due to the diversity of the surface cover in each area.

A detailed analysis of the surface spectral reflectance over urban areas requires a high spatial resolution due to the heterogeneity of its surface cover. The National Consortium on Remote Sensing in Transportation (NCRST) from the University of California, Santa Barbara (<http://www.ncgia.ucsb.edu/ncrst/resources/easyread/HyperCenterlines/first.html>), using the Airborne Visible InfraRed Imaging Spectrometer (AVIRIS) data, performed a detailed classification of the surface reflectance over Santa Barbara and Goleta urban area and identified distinct surface types. Further analysis was also performed by Herold et al. (2003) using AVIRIS data for 2000. The surface reflectance of several surface types was derived by taking advantage of the AVIRIS high spatial resolution (4 m) and 224 continuous spectral bands (0.40 to  $2.50 \mu\text{m}$ ). The analyzed surfaces include several vegetation types, soil and urban materials (asphalted or concreted roads, parking lots, roofs). The authors distinctively selected only homogeneous scenes in their analyses in order to characterize the specific targets since the 4 m resolution can still have a mix of different surface materials or shadows. Using their spectral data library categorized by different surface types, we computed the  $\rho_{\text{surf}}(0.66 \mu\text{m})/\rho_{\text{surf}}(2.1 \mu\text{m})$  ratio and plotted it against the  $\rho_{\text{surf}}(0.66 \mu\text{m})$  as illustrated in Fig. 3.

Results of the analysis from the Mexico City AERONET site at UNAM for the period of 2002–2005 are also plotted in Fig. 3. Each point represents a pixel of  $1.5 \text{ km} \times 1.5 \text{ km}$  spatial resolution from a 10 km box centered on the AERONET site and averaged over 6 and 8 days (Aqua and Terra respec-

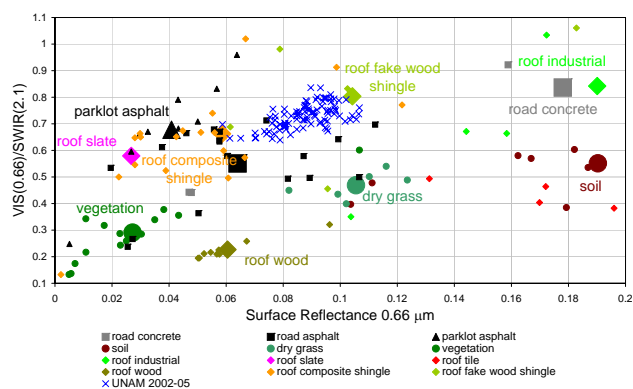


**Fig. 3.** The ratio between the  $\text{VIS}(0.66 \mu\text{m})/\text{SWIR}(2.1 \mu\text{m})$  is presented as a function of the surface reflectance at  $0.66 \mu\text{m}$ , based on the Herold et al. (2003) spectral library. Results from our MODIS analyses are also presented for data analyzed between 2002 and 2005 at 1.5 km resolution over a 10 km box centered on the AERONET site at UNAM in Mexico City.

tively), with  $\tau_a < 0.2$  and scattering angle  $< 140^\circ$ . Overall, Fig. 3 shows a positive dependence of the  $\rho_{\text{surf}}(0.66 \mu\text{m})/\rho_{\text{surf}}(2.1 \mu\text{m})$  ratio on the absolute surface reflectance at  $0.66 \mu\text{m}$ . From the natural surface data it is clear that going from green vegetated surfaces to non-photosynthetic vegetation like dry grass, and through to soils, there is an increase in the red reflectance and at the same time an increase in the reflectance ratio ranging on average from 0.3 to 0.5. The reflectivity in the visible blue and red wavelengths is lower for vegetated surfaces due to chlorophyll absorption. The short-wave infrared radiation is absorbed due to vibrational absorptions by liquid water and leaf components such as lignin and cellulose (Roberts et al., 1993; Kaufman et al., 2002). Drier and less photosynthetically active vegetation contribute to increase in the brightness at  $0.66 \mu\text{m}$  and  $2.1 \mu\text{m}$ . This signal is stronger for  $0.66 \mu\text{m}$  causing an increase in the ratio  $\rho_{\text{surf}}(0.66 \mu\text{m})/\rho_{\text{surf}}(2.1 \mu\text{m})$  as shown in Fig. 3.

Regarding the urban scenes, the roads and most of the roofs, even for low red reflectance, show systematically higher reflectance ratios of around 0.7. Our results for Mexico City at  $1.5 \text{ km} \times 1.5 \text{ km}$  resolution in the area surrounding the UNAM site show  $\rho_{\text{surf}}(0.66 \mu\text{m})/\rho_{\text{surf}}(2.1 \mu\text{m})$  ratios that vary from 0.60 up to 0.80 and surface reflectances at  $0.66 \mu\text{m}$  varying from 0.06 up to 0.11. This high variability reflects the heterogeneity of the surface cover in the 10-km box. In this area, there is a diversity of building rooftops, vegetated areas, and roads. The results from this work for each  $1.5 \text{ km} \times 1.5 \text{ km}$  pixel already represent a mix of different surface types and on average appear to be reasonably well explained by the reflectances of individual materials in the urban area. In particular, the urban mix of surface covers (asphalt, roof fake-wood shingle, concrete, etc.) shows reflectance ratios that are higher than the natural land covers (vegetation, dry grass, soil, etc.).

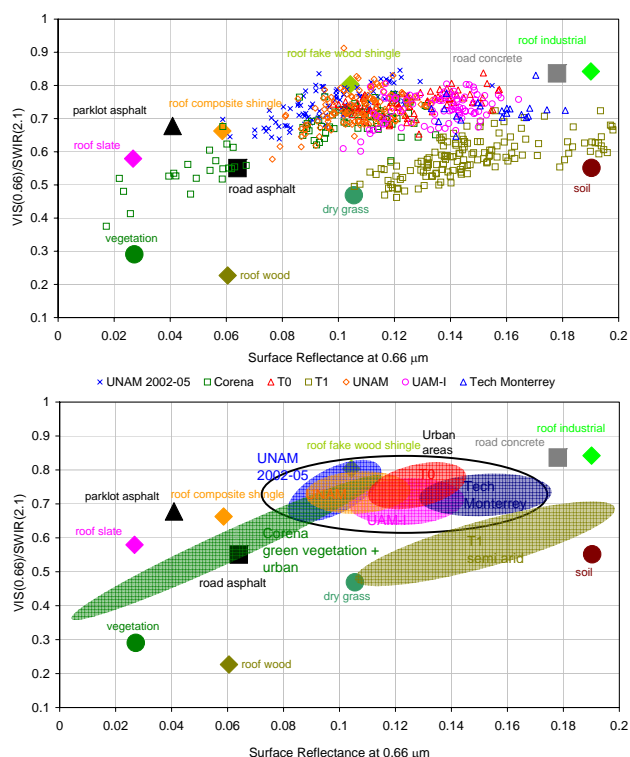


**Fig. 4.** (a) Same as Fig. 3 but including results from our MODIS analyses at  $1.5\text{ km} \times 1.5\text{ km}$  in a  $10\text{ km} \times 10\text{ km}$  box centered on each sun-photometer that operated during the MILAGRO Campaign in Mexico City in 2006; (b) Qualitatively illustrated clusters of the results from each measurement site.

Figure 4a repeats Fig. 3 but includes results from the sun-photometer network operated during the MILAGRO experiment. Figure 4b qualitatively shows the clustering of the different surface types as urbanized, semi arid and vegetated areas. Applying the same procedures as before, we considered only the cases where  $\tau_a < 0.2$ , but included all the cases independent of their scattering angles, to increase the statistics. The correction for the aerosol layer was applied using the  $\tau_a$  measured from all the sun-photometers in the network in the corresponding areas with one aerosol model used for the whole region. Each point corresponds to a pixel of  $1.5\text{ km}$  spatial resolution over an area of  $10\text{ km} \times 10\text{ km}$  centered on each of the sun-photometer sites.

It is important to note that surface properties obtained at the UNAM2006 site with the Microtops II, reconfirm those obtained with AERONET at the same site during 2002–2005, showing the consistency of the data. Like UNAM, the UAM-I, T0, and TEC sites represent urbanized areas with a high heterogeneity of surface cover. Overall, the urbanized sites show an average  $\rho_{\text{surf}}(0.66)/\rho_{\text{surf}}(2.1)$  value close to 0.73, in agreement with the value retrieved from the 2002–2005 data. The results from the different urbanized areas are somewhat different from each other, but detailed analyses of each re-

gion would be necessary to explain the differences seen in Fig. 4.

The Corena site is located at the southwest of UNAM in a vegetated park area; part of the  $10\text{ km} \times 10\text{ km}$  box includes urban areas as well as some part of the UNAM area. The Corena results in Fig. 4 are in good agreement with expectations from its mix of urban and vegetation characteristics, (i.e., the pixels that show lower reflectance ratios and lower surface reflectance at  $0.66\text{ }\mu\text{m}$  are in agreement with vegetated surface characteristics).

The T1 site is another representative site, which is located  $30\text{ km}$  northeast of Mexico City in a very arid area consisting of dry grass and exposed soil. The T1 results presented in Fig. 4 show good agreement with the surface composition of the area (i.e., values range between the dry grass and soil types with lower ratios and higher surface reflectance at  $0.66\text{ }\mu\text{m}$ ).

The surface ratios estimated from the sun-photometer measurements during MCMA-2006 Study presented different surface properties that were in agreement with the reference library of surface types in an urban area.

## 6 Aerosol optical depth computation

We obtained aerosol optical depth ( $\tau_a$ ) retrievals at  $1.5\text{ km}$  resolution based on MODIS Level 1B calibrated TOA reflectance at  $0.66$  and  $2.1\text{ }\mu\text{m}$ . The TOA reflectance at  $2.1\text{ }\mu\text{m}$  was used to estimate the surface reflectance at  $0.66\text{ }\mu\text{m}$  (Kaufman et al., 1997a) based on the  $\rho_{\text{surf}}(0.66)/\rho_{\text{surf}}(2.1)$  ratio estimated for the Mexico City urban area in this work. The aerosol optical model used was determined specifically for Mexico City as described in Sect. 4. The retrieval is based on a lookup equation that relates the TOA reflectance (at  $0.66\text{ }\mu\text{m}$ ) to an aerosol optical depth (at  $0.55\text{ }\mu\text{m}$ ), for a given surface reflectance, aerosol optical model, and satellite and solar geometries. The AOD at  $0.55\text{ }\mu\text{m}$  is extrapolated to  $0.66\text{ }\mu\text{m}$  and used for the computation of the TOA reflectance at this wavelength. The extrapolation of the AOD is based on the spectral dependence of the aerosol optical properties that we assumed based on the AERONET measurements. The lookup equations were defined based on simulations of the TOA reflectance for several aerosol optical depths using SB-DART under the relevant conditions (surface reflectance, geometry, water vapor amount).

Even with the observed variability between the different regions, and from one day to another, when averaged over  $10\text{ km} \times 10\text{ km}$  the  $\rho_{\text{surf}}(0.66)/\rho_{\text{surf}}(2.1)$  reflectance ratio is around 0.73 for scattering angles smaller than  $140^\circ$ . The use of this urban ratio, compared to a mean 0.56 ratio used for MODIS operational retrieval globally, can make a large difference in the  $\tau_a$  computation from satellite observations. Figure 5 presents the comparison between the computed  $\tau_a$  retrieved in this study with MODIS data and the measured  $\tau_a$  from AERONET in 2002–2005 and the hand-held sun-



photometer network during MCMA- 2006 Study. The ratio was defined based on the 2002–2005 data, but the results shown here are meant to demonstrate the effect that it can produce in the  $\tau_a$  estimation for the same period, and just confirmed for the independent period of 2006. In Fig. 5a the  $\tau_a$  was retrieved using the surface reflectance ratio of  $\rho_{\text{surf}}(0.66 \mu\text{m})/\rho_{\text{surf}}(2.1 \mu\text{m})=0.56$  and in Fig. 5b the retrieval was based on  $\rho_{\text{surf}}(0.66 \mu\text{m})/\rho_{\text{surf}}(2.1 \mu\text{m})=0.73$ . The comparison between the two plots shows a great improvement in Fig. 5b of the offset in Fig. 5a that was caused by inaccurate information on surface reflectance. It should be pointed out that the use of a mean aerosol optical model defined from AERONET data in this study was sufficient to represent the aerosol content in all analyses. This is verified by the precise slope of the fit being close to unity.

## 7 Conclusions

Based on the analysis of satellite and ground-based measurements in different urban sites in Mexico City, it can be deduced that even with the high heterogeneity of the surface, the average ratio of  $\rho_{\text{surf}}(0.66)/\rho_{\text{surf}}(2.1)=0.73\pm 0.06$  in a  $10 \text{ km} \times 10 \text{ km}$  area is representative of the urbanized surfaces for scattering angles smaller than  $140^\circ$  and  $0.77\pm 0.06$  for larger scattering angles. This was significantly different for a non-urban site T1, whose value of around 0.55 was in agreement with the expected value for dry grass and soil surfaces. Comparison between the  $10 \text{ km} \times 10 \text{ km}$   $\tau_a$  averages (retrieved from MODIS at  $1.5 \text{ km}$  resolution) and 1-h averages from the sun-photometers observed for each of the measurement sites shows a significant improvement in the  $\tau_a$  estimation for the 2006 independent data set, when using the new surface ratio (0.73). This result shows that for  $\tau_a$  retrieval at  $10 \text{ km} \times 10 \text{ km}$  spatial resolution the surface ratio assumption (0.73) is good for the analyzed urban area. However, at higher spatial resolutions such as  $1.5 \text{ km}$ ,  $\tau_a$  retrieval would need to consider a flexible  $\rho_{\text{surf}}(0.66)/\rho_{\text{surf}}(2.1)$  ratio for each single pixel, as we found a high variability in the ratio (0.60–0.80) at  $1.5 \text{ km}$ .

This paper demonstrates that the  $\rho_{\text{surf}}(0.66)/\rho_{\text{surf}}(2.1)$  ratio of  $0.73\pm 0.06$  obtained for the Mexico City urban area is larger than the value used globally in the MODIS operational algorithm due to urbanization. If this value is not considered, satellite AOD retrieval over Mexico City can incur significant overestimation. The same may happen over other urban areas, as this ratio strongly depends on the level of urbanization, particularly the urban to vegetation proportions and the types of surface materials. Therefore, we strongly encourage similar analyses in other urban areas to enhance the development of a parameterization of surface ratios that account for urban heterogeneities. Knowledge of urban surface reflectance ratios is essential for accurate retrieval of AOD from satellite over such surfaces. Satellite retrieval of AOD over urban areas has become extremely important as urban-

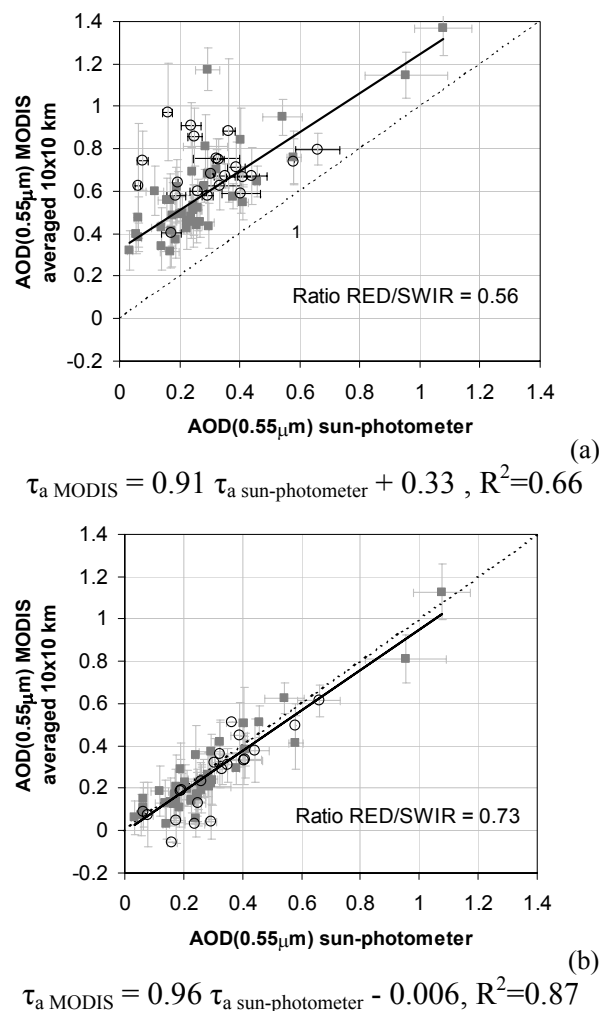


**Fig. 5.** Aerosol optical depth ( $\tau_a$ ) retrieved from MODIS reflectance data in this study at  $1.5 \text{ km} \times 1.5 \text{ km}$  resolution and averaged over  $10 \text{ km} \times 10 \text{ km}$  around the sun-photometer site, compared to  $\tau_a$  measured with the sun-photometers averaged over one hour around the satellite overpass time, for  $\rho_{\text{surf}}(0.66 \mu\text{m})/\rho_{\text{surf}}(2.1 \mu\text{m})$  values of (a) 0.56 and (b) 0.73. Squares represent data from 2002–2005 from the AERONET at UNAM, and open circles represent data from the sun-photometer network that operated during the MILAGRO Campaign in 2006. The error bars represent their respective standard deviations.

ization increases exponentially worldwide. Progress in this domain will provide an alternative tool to complement the routine monitoring of urban air-pollution control efforts.

**Acknowledgements.** This work was supported by a Molina Fellowship in Environmental Science (to A. D. de A. Castanho) and Department of Energy grant DE-FG02-05ER63980. We are very grateful for the innumerable helpful participation of the following students that worked on this project operating the MicrotopsII supported by INE (Instituto Nacional de Ecología): F. Ramirez Hernandez, I. Vega del Valle, P. A. Hernandez Priego, G. V. Valdes, A. Arraiga and L. D. Reyes Cortes. We also acknowledge the

AERONET site managers at Mexico City A. Leyva, Technician H. R. Estévez from the Institute of Geophysics at UNAM and the AERONET global PI, B. Holben, for making available an extensive and high quality aerosol data set. We also thank G. Sosa for logistical support at the IMP – T0. We acknowledge L. Remer and R. Levy for valuable discussions, as well as C. Gatebe and two anonymous reviewers for their helpful comments.

Edited by: S. Madronich

## References

- Al-Saadi, J., Szykman, J., Pierce, R. B., et al.: Improving national air quality forecasts with satellite aerosol observations, *Bull. Am. Meteorol. Soc.*, 86(9), 1249–1264, 2005.
- Castanho, A. D. A., Martins, J. V., Hobbs, P. V., Artaxo, P., Remer, L., and Yamasoe, M. A.: Chemical characterization of aerosols on the East Coast of the United States using aircraft and ground based stations during the CLAMS Experiment, *J. Atmos. Sci.*, 62, 934–946, 2005.
- Li, C., Lau, A. K. H., Mao, J., and Chu, A.: Retrieval, Validation, and Application of the 1-km Aerosol Optical Depth From MODIS Measurements Over Hong Kong, *IEEE Trans. Geosci. Remote Sens.*, 43(11), 2650–2658, 2005.
- Dubovik, O. and King, M. D.: A flexible inversion algorithm for retrieval of aerosol optical properties from sun and sky radiance measurements, *J. Geophys. Res.*, 105(D16), 20 673–20 696, 2000.
- Dubovik, O., Holben, B., Eck, T. F., Smirnov, A., Kaufman, Y. J., King, M. D., Tanré, D., and Slutsker, I.: Variability of absorption and optical properties of key aerosol types observed in worldwide locations, *J. Atmos. Sci.*, 59, 590–608, 2002.
- Gatebe, C. K., King, M. D., Tsay, S., Ji, Q., Arnold, G. T., and Li, J. Y.: Sensitivity of off-nadir zenith angles to correlation between visible and near-infrared reflectance for use in remote sensing of aerosol over land, *IEEE Trans. Geosci. Remote Sens.* 39(4), 805–819, 2001.
- Gross, B., Ogunwuyi, O., Moshary, F., Ahmed, S.; Cairns, B.: MODIS aerosol retrieval over urban areas, *Atmospheric and Environmental Remote Sensing Data Processing and Utilization: Numerical Atmospheric Prediction and Environmental Monitoring*, edited by: Huang, H.-L. A., Bloom, H. J., Xu, X., and Dittberner, G., *J. Proceedings of the SPIE*, 5890, 274–283, 2005.
- Guenther, B., Xiong, X., Salomonson, V. V., Barnes, W. L., and Young, J.: On-orbit performance of the Earth Observing System Moderate Resolution Imaging Spectroradiometer: First year of data, *Remote Sens. Environ.*, 83, 16–30, 2002.
- Herold, M., Gardner, M., and Roberts, D. A.: Spectral Resolution Requirements for Mapping Urban Areas, *IEEE Transactions on Geoscience and Remote Sensing*, 41(9), 1907–1919, 2003.
- Holben, B. N., Tanre', D., and Smirnov, A.: An emerging ground-based aerosol climatology: Aerosol Optical depth from AERONET, *J. Geophys. Res.*, 106(D11), 12 067–12 097, 2001.
- Ichoku, C., Chu, D. A., Mattoo, S., Kaufman, Y. J., Remer, L. A., Tanré, D., Slutsker, I., and Holben, B. N.: A spatiotemporal approach for global validation and analysis of MODIS aerosol products, *Geophys. Res. Lett.*, 29, 8006, doi:10.1029/2001GL013206, 2002a.
- Ichoku, C., Levy, R., Kaufman, Y. J., et al.: Analysis of the performance characteristics of the five-channel Microtops II sun-photometer for measuring aerosol optical thickness and precipitable water vapor, *J. Geophys. Res.*, 107, 4179, doi:10.1029/2001JD001302, 2002b.
- Kaufman, Y.J., Tanré, D., Gordon, H. R., et al.: Passive remote sensing of tropospheric aerosol and atmospheric correction for the aerosol effect, *J. Geophys. Res.*, 102(D14), 16 815–16 830, 1997a.
- Kaufman, Y.J., Tanré, D., Remer, L. A., Vermote, E. F., Chu, A., and Holben, B.: Operational remote sensing of tropospheric aerosol over land from EOS moderate resolution imaging spectroradiometer, *J. Geophys. Res.*, 102, 17 051–17 067, 1997b.
- Kaufman, Y. J., Gobron, N., Pinty, B., Widlowski, J., and Verstraete, M. M.: Relationship between surface reflectance in the visible and mid-IR used in MODIS aerosol algorithm – theory, *J. Geophys. Res.*, 29(23), 2116, doi:10.1029/2001GL014492, 2002.
- King, M. D., Menzel, W. P., Kaufman, Y.J., Tanré, D., Gao, B. C., Platnick, S., Ackerman, S. A., Remer, L. A., Pincus, R., and Hubanks, P. A.: Cloud and aerosol properties, precipitable water, and profiles of temperature and water vapor from MODIS, *IEEE Trans Geosci. Remote Sens.*, 41(2), 442–458, 2003.
- Levy, R. C., Remer, L. A., and Kaufman, Y. J.: Effects of neglecting polarization on the MODIS aerosol retrieval over land, *IEEE Trans. Geosci. Rem. Sens.*, 42(11), 2576–2583, 2004.
- Levy, R. C., Remer, L. A., Martins, J. V., and Kaufman, Y. J.: Evaluation of the MODIS aerosol retrievals over ocean and land during CLAMS experiment, *J. Atmos. Sci.-Special Sect.*, 62, 974–992, 2005.
- Levy, R. C., Remer, L. A., Matto, S., Vermote, E. F., and Kaufman, Y. J.: Second-generation operational algorithm: Retrieval of aerosol properties over land from inversion of Moderate Resolution Imaging Spectroradiometer spectral reflectance, *J. Geophys. Res.*, 112, D13211, doi:10.1029/2006JD007811, 2007.
- Martins, J. V., Tanré, D., Remer, L. A., Kaufman, Y., Mattoo, S., and Levy, R.: MODIS cloud screening for remote sensing of aerosols over ocean using spatial variability, *Geophys. Res. Lett.*, 29(12), doi:10.1029/2001GL013252, 2002.
- Meister, G.: Bidirectional Reflectance of Urban Surfaces, PhD thesis, University of Hamburg, II, Institut für Experimentalphysik, 186, URL: <http://kogs-www.informatik.uni-Hamburg.de/PROJECTS/censis/publications.html>, 2000.
- Morys, M., Mims III, F. M., Hagerup, S., Anderson, S. E., Baker, A., Kia, J., and Walkup, T.: Design, calibration, and performance of MICROTOS II handheld ozone monitor and sun-photometer, *J. Geophys. Res.*, 106, 14 573–14 582, 2001.
- Parkinson, C. L.: Aqua: An Earth-Observing Satellite Mission to Examine Water and Other Climate Variables, *IEEE Transactions on Geoscience and Remote Sensing*, 41(2), 173–183, 2003.
- Remer, L. A., Wald, A. E., and Kaufman, Y.: Angular and seasonal variation of spectral surface reflectance ratios: Implications for the remote sensing of aerosol over land, *IEEE Trans. Geosci. Remote Sens.*, 39(2), 275–283, 2001.
- Remer, L.A., Kaufman, Y. J., Tanre, D., et al.: The MODIS Aerosol Algorithm, products, and validation, *J. Atmos. Sci.-Special Edition*, 62, 947–973, 2005.
- Ricchiazzi, P., Yang, S., Gautier, C., and Sowle, D.: SBDART: A Research and Teaching Software Tool for Plane-Parallel Radiative Transfer in the earth's Atmosphere, *Bull. Am. Meteorol.*

- Soc., 79, 2101–2114, 1998.
- Roberts, D. A., Smith, M. O., and Adams, J. B.: Green Vegetation, Nonphotosynthetic Vegetation, and soils in AVIRIS Data, *Remote Sensing of Environment*, 44(2–3), 255–269, 1993.
- Salcedo, D., Onasch, T. B., Dzepina, K., et al.: Characterization of ambient aerosols in Mexico City during the MCMA-2003 campaign with Aerosol Mass Spectrometry: results from the CENICA Supersite, *Atmos. Chem. Phys.*, 6, 925–946, 2006, <http://www.atmos-chem-phys.net/6/925/2006/>.
- Vermote, E. F., Tanré, D., Deuze, J. L., et al.: Second Simulation of the Satellite Signal in the Solar Spectrum, 6S: An overview, *IEEE Trans. Geosci. Remote Sens.*, 35(3), 675–686, 1997.